Running head:

Epigenetic Regulation of Defense Pathway

Corresponding author:

Wen-Hui Shen

Institut de Biologie Moléculaire des Plantes du CNRS

Université de Strasbourg

12 rue du Général Zimmer

67084 Strasbourg Cedex

France

Phone +33 3 88 41 72 83

Fax +33 3 88 61 44 42

email Wen-Hui.Shen@ibmp-cnrs.unistra.fr

Arabidopsis Histone Methyltransferase SDG8 Mediates Induction of the Jasmonate/Ethylene-Pathway Genes in Plant Defense Response to Necrotrophic Fungi [1]

Alexandre Berr, Emily J. McCallum[2], Abdelmalek Alioua, Dimitri Heintz, Thierry Heitz and Wen-Hui Shen*

Institut de Biologie Moléculaire des Plantes du CNRS, Université de Strasbourg, 12 rue du Général Zimmer, 67084 Strasbourg Cedex, France

Footnotes:

[2]Present address: Department of Biology, Plant Biotechnology, ETH Zürich, Universitätstrasse 2, 8092 Zürich, Switzerland

*Corresponding author; e-mail Wen-Hui.Shen@ibmp-cnrs.unistra.fr; fax 33 3 88 61 44 42.

ABSTRACT

As sessile organisms, plants have to endure a wide variety of biotic and abiotic stresses, and accordingly have evolved intricate and rapidly inducible defense strategies associated with the activation of a battery of genes. Among other mechanisms, changes in chromatin structure are thought to provide a flexible, global and stable means for regulation of gene transcription. In support of this idea, we demonstrate here that the *Arabidopsis thaliana* histone-methyltransferase SET DOMAIN GROUP8 (SDG8) plays a crucial role in plant defense against fungal pathogens by regulating a subset of genes within the jasmonic acid (JA) and/or ethylene (ET) signaling pathway. We show that the loss-of-function mutant *sdg8-1* displays reduced resistance to the necrotrophic fungal pathogens *Alternaria brassicicola* and *Botrytis cinerea*. While levels of JA, a primary phytohormone involved in plant defense, and camalexin, a major phytoalexin against fungal pathogens, remain unchanged or even above normal levels in *sdg8-1*, induction of several defense genes within the JA/ET signaling pathway is severely compromised in response to fungal infection or JA treatment in mutant plants. Both downstream genes and, remarkably, also upstream MAPK-kinase genes *MKK3* and *MKK5* are misregulated in *sdg8-1*. Accordingly, chromatin immunoprecipitation analysis shows that *sdg8-1* impairs dynamic changes of H3K36 methylation at defense marker genes as well as at *MKK3* and *MKK5*, which normally occurs upon infection with fungal pathogens or methyl-JA treatment in wild-type plants. Our data indicates that SDG8-mediated H3K36 methylation may serve as a memory of permissive transcription for a subset of defense genes allowing rapid establishment of transcriptional induction.

INTRODUCTION

To compensate for their sessile nature, plants have evolved intricate and diverse strategies enabling them to survive and adapt to a broad range of biotic stresses, including insect, herbivore and pathogen attacks. Plant resistance or tolerance to biotic stresses is mediated via pre-existing physical and chemical barriers as well as rapidly inducible defense mechanisms. Induction of basal defenses is triggered by perception of conserved pathogen-associated molecular patterns (PAMPs), whereas more specific microbial effectors elicit *gene-for-gene* resistance responses (Jones and Dangl, 2006). In both cases, induction of the antimicrobial arsenal (Ferreira et al., 2007) depends in part on phytohormone signaling, including mediation by salicylic acid (SA), jasmonic acid (JA) and ethylene (ET) (Glazebrook, 2005). In general, activation of SA-dependent responses, including systemic acquired resistance, is most efficient against biotrophic pathogen attacks, whereas responses mediated by JA and ET are more prominent following infection with necrotrophic pathogens. Transcriptome analysis of *Arabidopsis* has demonstrated that the characteristic signaling network of each plant-attacker combination orchestrates very complex and wide ranging transcriptional reprogramming, ultimately leading to increased plant resistance (Glazebrook et al., 2003; De Vos et al., 2005). Among the mechanisms capable of such rapid and broad reprogramming of gene expression, the role that chromatin remodeling plays in response to changing environmental cues has received little attention until now.

Histone variants and post-translational modification (e.g. acetylation, methylation, phosphorylation) of histone tails form the so-called histone code (Strahl and Allis, 2000; Turner, 2000), in which chromatin remodeling establishes a rapid and reversible differential pattern of gene expression across the genome. In euchromatin, methylation of histone H3 lysine 4 (H3K4) and H3K36 is associated with transcriptional activation, whereas

trimethylation of H3K27 (H3K27me3) is associated with gene silencing. These active and repressive methylation marks are established by the evolutionarily conserved SET [named after SuVar(3-9), E(z) and Trithorax] domain protein of the Trithorax-Group (TrxG) and Polycomb Group (PcG), respectively. The role of TrxG/PcG factors in the regulation of plant homeotic genes and developmental processes has been extensively studied (reviewed in Pien and Grossniklaus, 2007; He, 2009; Shen and Xu, 2009). More recent studies have shown that changes in histone methylation also occur under stress conditions. In *Arabidopsis*, changes in histone modification patterns (e.g. enrichment in H3K4me3) were observed at several genes in response to drought stress (Kim et al., 2008). H3K27me3 was decreased in the chromatin of *COR15A* and *ATGOLS3* during cold exposure and remained at low levels after returning to normal growth conditions (Kwon et al., 2009). ATX1, a TrxG member involved in H3K4 trimethylation (Alvarez-Venegas and Avramova, 2005) was shown to be necessary for induction of *WRKY70*, a transcription factor gene in the SA-pathway involved in defense against bacterial pathogen (Alvarez-Venegas et al., 2007).

The *SET DOMAIN GROUP8* (*SDG8*, also named *EFS, ASHH2*, and *CCR1*) gene is a yeast *SET2* and *Drosophila ASH1* homolog and its mutations cause pleiotropic plant phenotypes, including early flowering (Kim et al., 2005; Zhao et al., 2005), reduced organ size and enhanced shoot branching (Dong et al., 2008; Xu et al., 2008), altered carotenoid composition (Cazzonelli et al., 2009), and reduced fertility (Grini et al., 2009). In *sdg8* mutants, H3K36me2 and H3K36me3 levels were reduced not only at specific loci but were also reduced in global histone extracts, suggesting that SDG8 may have additional uncharacterized functions. In the present work, we provide evidence that *SDG8* plays crucial roles in plant defense against necrotrophic fungal pathogens through H3K36me3-mediated activation of a subset of genes within the JA/ET signaling defense pathway.

RESULTS

***SDG8* promoter activity is induced by wounding and fungal pathogen infection**

Previous reverse transcription (RT)-PCR analysis has shown that *SDG8* is ubiquitously expressed in different plant organs and *in situ* hybridization revealed a higher abundance of *SDG8* transcripts in actively dividing tissues, such as the ovule primordia and shoot apical meristem (Zhao et al., 2005). Here, we examined spatial expression patterns in transgenic plants using a β-glucuronidase reporter gene driven by 2655 bp of the *SDG8* promoter (*SDG8p::GUS*). T2 progeny from three independent primary transformants were examined for GUS expression by histochemical staining. All three transgenic lines display a largely similar expression pattern and hereinafter data from one representative line (Line A) is shown. In 8-day-old seedlings, GUS activity was detected in root tips and stipules (Fig. 1A and 1B). In true leaves, strong GUS activity was observed in hydathodes at the leaf margin (Fig. 1C) and at the base of cauline leaves from both primary and secondary stems (Fig. 1D). In flowers, GUS staining was observed in anther vasculature (Fig. 1E), the transmitting tract of the upper part of the pistil, and at the base of pistil following abscission of sepals and petals (Fig. 1F). These tissue-specific expression patterns are relatively distinct from the previous report using a shorter version of *SDG8* promoter fused with *GUS* (Cazzonelli et al., 2010) but are more similar to those reported for a *GUS* fusion at the 3'-end of the *SDG8* gene (Kim et al., 2005), indicating that multiple *cis*-elements exist in regulating *SDG8* expression.

In addition, *SDG8p::GUS* expression was inducible in response to stress. Upon mechanical wounding, strong GUS activity was observed along the cut edge of tissues (Fig. 1G). When leaves of transgenic plants were spot-inoculated with *Botrytis cinerea* or *Alternaria brassicicola*, both necrotrophic fungal pathogens, strong GUS staining was observed in the tissue bordering inoculation sites and in tissues more distant from the

inoculation site (Fig. 1H and 1I). Similar results were obtained in three independent transgenic *SDG8p::GUS* lines and negative controls did not show obvious induction of GUS expression (see Supplemental Fig. S1 online). Quantitative RT-PCR analysis showed that *SDG8* expression was significantly induced ($P<0.05$ in two-sided *t*-test; see Supplemental Table S1 online) following fungal infection of wild-type Columbia (Col) plants (Fig. 1J), confirming the results observed in the *GUS* reporter lines.

The *sdg8-1* mutant shows reduced resistance to fungal pathogen infection

The finding that *SDG8* expression is inducible in response to fungal pathogens, together with the fact that pathogen-responsive genes are over-represented in the previously generated list of down-regulated genes in *sdg8* mutant seedlings (Xu et al., 2008; Supplemental Fig. S2) prompted us to investigate the role of *SDG8* in pathogen defense. We compared the *sdg8-1* mutant with wild-type plants in order to study their respective resistance to infection with the fungi *B. cinerea* and *A. brassicicola*.

Rosette leaves of 6-week-old soil-grown plants were challenged with *B. cinerea* by inoculation of a fungal spore suspension onto small holes made using a needle. Lesions caused by *B. cinerea* infection were readily visible on wild-type Col and *sdg8-1* and *sdg8-2* leaves at 3 days post-inoculation (dpi). Nevertheless, these lesions developed more extensively in mutant plants, eventually affecting the entire leaf blade (Fig. 2A). Previous studies have established that *sdg8-1* and *sdg8-2* are allelic mutants and that loss-of-function of SDG8 causes the previously described mutant phenotypes (Kim et al., 2005; Zhao et al., 2005; Dong et al., 2008; Xu et al., 2008; Cazzonelli et al., 2009; Grini et al., 2009). Consistently, the *sdg8-1* and *sdg8-2* mutants show similar disease symptoms (Fig. 2A). Hereinafter, we concentrated on *sdg8-1* for detailed studies. The size of lesions caused by *B. cinerea* were approximately 3 times larger in the *sdg8-1* mutant compared to those on Col

leaves (Fig. 2B). Enhanced fungal growth was apparent in *sdg8-1* (Fig. 2C) and quantitative PCR (qPCR) analysis further confirmed higher levels of fungal multiplication in *sdg8-1* compared to Col (Fig. 2D, Supplemental Fig. S3A), which correlate with the increased severity of disease symptoms.

A. brassicicola inoculation was performed by application of a fungal spore suspension directly onto intact leaf surfaces. In Col, disease symptoms were limited to tiny necrotic spots at the site of inoculation. In contrast, *sdg8-1* leaves displayed severe necrotic symptoms that turned a purplish color (Fig. 2E), with a dramatic 5-fold increase in average lesion diameter compared to Col at 5 dpi (Fig. 2F). Enhanced fungal growth in *sdg8-1* was also apparent from qPCR analysis of infected leaf tissue (Fig. 2G, Supplemental Fig. S3B).

Taken together, these results indicate that *SDG8* is required for resistance to the fungal pathogens *B. cinerea* and *A. brassicicola* in *Arabidopsis*.

The JA/ET defense pathway is compromised in the *sdg8-1* mutant

We next investigated the molecular mechanisms associated with reduced resistance of *sdg8-1* plants to fungal infection. It has been reported that resistance to necrotrophic fungal pathogens in plants is strongly dependent upon the production of camalexin, an indole-type phytoalexin (Thomma et al., 1999). We therefore compared camalexin accumulation in *sdg8-1* and Col plants in response to *A. brassicicola* infection. Prior to inoculation, basal levels of camalexin were similarly low in *sdg8-1* and Col plants (Fig. 3A). Upon infection, *sdg8-1* plants retained a strong capacity to accumulate camalexin, and levels in mutant plants were approximately two times higher than in Col plants at 5 dpi (Fig. 3A). The increased accumulation of camalexin at later stages of infection may reflect more extensive tissue colonization by *A. brassicicola* in the *sdg8-1* plants. In any case, we did not detect any

reduction in camalexin synthesis which would explain the reduced resistance to fungal infection as observed in the *sdg8-1* mutant.

Activation of the JA/ET-dependent defense pathway, also required for resistance to necrotrophic pathogens (Thomma et al., 1998; Glazebrook et al., 2003), results in induction of the downstream defense genes *PDF1.2a* and *VSP2* (Fig. 3B). We analyzed *PDF1.2a* and *VSP2* expression in order to determine if the JA/ET defense pathway response is perturbed in the *sdg8-1* mutant. Interestingly, *sdg8-1* plants showed a reduction in basal expression levels of *PDF1.2a* compared to Col, while *VSP2* levels remained relatively unchanged (Fig. 3C, Supplemental Table S2). In response to *A. brassicicola* infection, *PDF1.2a* and *VSP2* induction was severely impaired in the *sdg8-1* mutant, which is in sharp contrast to their strong induction in Col plants (Fig. 3C, Supplemental Table S2). Similar defects in the induction of *PDF1.2a* and *VSP2* expression were also observed in *sdg8-1* following inoculation with *B. cinerea* (Supplemental Fig. S4 and Table S3). These results suggest that the JA/ET defense signaling pathway is compromised in *sdg8-1* plants, likely resulting in their reduced capacity to defend against fungal pathogens.

SDG8 is an essential activator required for induction of a subset of genes of the JA/ET defense pathway

To determine more precisely which aspects of the JA/ET signaling pathway are affected in *sdg8-1*, JA levels in methanolic extracts of Col and *sdg8-1* plants were measured before and after *A. brassicicola* inoculation. Basal JA levels were comparable in Col and *sdg8-1* at 0 dpi, and a significant and similar increase in JA accumulation occurred at 5 dpi (Fig. 4A). Thus, JA biosynthesis/accumulation in response to fungal attack is unaffected in *sdg8-1*. We next examined gene expression profiles in response to exogenously applied methyl-JA (MeJA) in *sdg8-1* and Col plants. *ERF1* and *MYC2*, encoding two transcription factors, are known to

control defense gene regulation in separate branches of the JA/ET signaling pathway (see Fig. 3B). MYC2 plays a pivotal role in the JA signaling pathway, and positively regulates JA- and wound/insect-responsive genes (e.g. *VSP2* and *LOX3*; Lorenzo et al., 2004). ERF1 plays a key role in integrating JA and ET signals, and positively regulates the pathogen-responsive genes *LOX2*, *PR4* and *PDF1.2a* (Lorenzo et al., 2003). Additionally, MYC2 and ERF1 exert antagonistic effects on each other's target genes, and thus provide the means to intricately regulate pathway dynamics in response to varying JA and/or ET input signals (Boter et al., 2004; Lorenzo et al., 2004). In Col plants, all examined genes (including *ERF1*, *MYC2*, *PDF1.2a*, *VSP2, LOX3, LOX2* and *PR4*) were rapidly induced, to varying extents, upon exposure to MeJA (Fig. 4B, Supplemental Fig. S5 and Table S4). Remarkably, the increase in *ERF1* and *MYC2* transcript levels was significantly lower in *sdg8-1* compared to Col plants, and an even more dramatic reduction was observed in their respective downstream target genes, *PDF1.2a* and *VSP2* after MeJA treatment (Fig. 4B, Supplemental Table S4). It is possible that the observed differences in inducible expression of JA/ET pathway genes is due to aberrant development and/or size differences between 6-week-old Col and *sdg8-1* plants, however similar results were also obtained following MeJA treatment of 10-day-old Col and *sdg8-1* seedlings of comparable size in two independent experiments (Supplemental Table S5). These results establish that *SDG8* is necessary for transcriptional activation of genes in both the *ERF1*- and *MYC2*-branches of the JA/ET signaling pathway.

SDG8-mediated H3K36 trimethylation is associated with induced expression of the defense marker genes *PDF1.2a* and *VSP2*

We hypothesized that JA treatment or pathogen attack may engender a massive transcriptional reprogramming in *Arabidopsis* through a global change in H3K36 trimethylation catalyzed by SDG8. We addressed this assumption by western blot analysis of changes in H3K36me1 and

H3K36me3 levels in Col plants following *A. brassicicola* infection or exogenous MeJA treatment. H3K36me1 was included in our analysis because this mark was previously shown to accumulate in *sdg8* mutants (Xu et al., 2008). Our results indicate that under the examined stresses, H3K36me1 and H3K36me3 levels remain relatively constant (Supplemental Fig. S6), indicating that JA treatment or fungal infection does not affect global levels of H3K36 methylation in *Arabidopsis*.

We next investigated gene locus-specific levels of H3K36me1 and H3K36me3 in order to better understand the molecular mechanisms underlying SDG8-mediated transcription activation of JA/ET defense pathway genes. Chromatin immunoprecipitation (ChIP) coupled with qPCR analysis was performed for *PDF1.2a* and *VSP2*, analyzing two regions of each gene. We chose these defense marker genes because they act at the most downstream steps of the JA/ET signaling pathway (see Fig. 3B) and thus provide interesting models to test whether their expression is directly or indirectly associated with SDG8-mediated H3K36 methylation. In unchallenged plants, levels of H3K36me3 at the chromatin regions of both *PDF1.2a* and *VSP2* were lower in *sdg8-1* compared to Col (Fig. 5, Supplemental Table S6). Upon fungal inoculation, the H3K36me3 levels were significantly increased in Col but were entirely unaffected in *sdg8-1*. In contrast, basal H3K36me1 levels were similar at *PDF1.2a* or slightly higher at *VSP2* in *sdg8-1* compared to Col, and fungal challenge decreased H3K36me1 levels at both *PDF1.2a* and *VSP2* in Col but not in *sdg8-1*. In comparison, H3K27me3 at *PDF1.2a* and *VSP2* were found at very low levels in both *sdg8-1* and Col and were unchanged following fungal infection (Fig. 5, Supplemental Table S6). The presence of only low levels of H3K27me3 at the chromatin of genes involved in defense against necrotrophic pathogens is likely to be beneficial for the plant as the likelihood of silencing is reduced. We also examined H3K36me3, H3K36me1 and H3K27me3 levels in response to MeJA treatment. Similar to *A. brassicicola* infection, *PDF1.2a* and *VSP2*

displayed increased H3K36me3, reduced H3K36me1 and unchanged H3K27me3 levels in response to MeJA treatment in Col, and changes in H3K36me3 and H3K36me1 were undetectable in *sdg8-1* (Supplemental Fig. S7 and Table S7). Taken together, these results indicate that dynamic changes in H3K36 methylation at *PDF1.2a* and *VSP2* occur in response to fungal infection and MeJA treatment, and show that SDG8-mediated H3K36me3 is directly associated with transcriptional induction of these defense genes. As previously proposed (Xu et al., 2008), H3K36me1 may be catalyzed by a different enzyme and defects in converting mono-methyl to di-/tri-methyl marks could result in elevated levels of H3K36me1 observed at these loci in *sdg8-1*.

SDG8 is required for transcriptional regulation of *MKK3* and *MKK5* involved in early steps of defense signaling

So far, our results have established that SDG8 is directly implicated in the activation of defense marker genes that exert functions at downstream steps in the JA/ET defense pathway. To further assess the molecular function of *SDG8* in pathogen defense, we investigated early genes in the defense-signaling pathway. Several mitogen-activated protein kinases (MAPKs) activate transcription factors involved in regulating defense gene expression (Pitzschke et al., 2009). The roles of MAPK kinases MKK4 and MKK5 in defense pathways are best characterized, and act as positive regulators of the ET pathway in response to pathogen infection, while MKK3 acts downstream of JA to repress *MYC2* expression (Takahashi et al., 2007; Pitzschke et al., 2009; also see Fig. 3B). *MKK5* expression was shown to be down-regulated in the *sdg8-1* and *sdg8-2* mutants in a previous microarray screen (Xu et al., 2008). We used qPCR to investigate the expression of *MKK5, MKK4* and *MKK3*, as well as *MKK2* and *MKK1,* which are involved in cold and drought stress responses, respectively (Teige et al., 2004; Xing et al., 2008). While basal expression levels of *MKK1, MKK2* and *MKK4* were

similar in *sdg8-1* and Col (Supplemental Fig. S8 and Table S2), a significantly reduced level of *MKK5* and increased level of *MKK3* were observed in *sdg8-1* (Fig. 6A, Supplemental Table S2). *MKK3* sequences are not present on the CATMA chip, and consequently *MKK3* expression data was not available from the previous microarray screen (Xu et al., 2008). Interestingly, in response to *A. brassicicola* infection, expression of *MKK3* and *MKK5* increased over the measured time period in Col but remained unchanged in *sdg8-1* (Fig. 6A, Supplemental Table S2), indicating a similar requirement of *SDG8*-dependent transcriptional regulation. In *sdg8-1* plants, the high basal level of *MKK3* was comparable to that of *A. brassicicola* infected Col plants, and *MKK3* expression in *sdg8-1* remained unchanged following fungal inoculation (Fig. 6A, Supplemental Table S2). In contrast, *MKK1* and *MKK2* expression was not responsive to fungal challenge, and the observed inducibility of *MKK4* expression occurred in an *SDG8*-independent manner in both Col and *sdg8-1* plants (Supplemental Fig. S8A and Table S2). MeJA treatment did not affect *MKK1*, *MKK2* or *MKK4* expression levels in either Col or *sdg8-1* mutant plants (Supplemental Fig. S8B and Table S4). Consistent with their respective position in the JA/ET defense signaling pathway (see Fig. 3B), *MKK3* but not *MKK5* expression was induced by MeJA treatment in Col (Fig. 6B, Supplemental Table S4). In *sdg8-1*, *MKK3* expression levels remained constantly high and *MKK5* constantly low following MeJA treatment (Fig. 6B, Supplemental Table S4).

To gain insight into the *SDG8*-dependent induction of *MKK3* and *MKK5* expression following *A. brassicicola* infection, we analyzed H3K36 methylation of these loci at three different regions by ChIP coupled with qPCR. In unchallenged plants, decreased levels of H3K36me3 accompanied by increased levels of H3K36me1 were detected at *MKK5*, particularly toward the 3'-end of the gene, in the *sdg8-1* mutant compared to Col plants (Fig. 6C, Supplemental Table S6). This result is consistent with the previously observed pattern of down-regulation of *SDG8*-dependent genes. In agreement with the basal up-regulation of

MKK3 expression in *sdg8-1*, H3K36me3 levels were increased and H3K36me1 decreased at *MKK3* chromatin regions in *sdg8-1* compared to Col (Fig. 6C, Supplemental Table S6). We speculate that SDG8 may share a limiting factor with another H3K36-methyltransferase complex more extensively involved in H3K36 trimethylation at the *MKK3* loci and, consequently, *SDG8*-knockdown results in enhanced *MKK3* transcription. Remarkably, despite the differences in basal H3K36 methylation observed in unchallenged plants, both *MKK5* and *MKK3* loci displayed increased H3K36me3 and decreased H3K36me1 in Col but not in *sdg8-1* mutant plants in response to fungal infection (Fig. 6C, Supplemental Table S6). Taken together, these results indicate that SDG8-mediated H3K36 methylation is directly involved in inducible expression of both *MKK3* and *MKK5* at early steps of the defense-signaling pathway against fungal pathogens.

DISCUSSION

Previous studies have established that *SDG8* and H3K36 methylation play important roles in several developmental processes (Kim et al., 2005; Zhao et al., 2005; Dong et al., 2008; Xu et al., 2008; Cazzonelli et al., 2009; Grini et al., 2009). In this study, we have demonstrated that *SDG8* and H3K36 methylation are involved in the establishment of a chromatin state required for inducible defense against necrotrophic fungal pathogens.

    sdg8-1 mutant plants display reduced resistance to the necrotrophic fungal pathogens *A. brassicicola* and *B. cinerea. sdg8-1* plants contain normal levels of camalexin, an important compound involved in anti-microbial defense against necrotrophic pathogens. *sdg8-1* plants also contain normal levels of JA, but are compromised in the inducible expression of a subset of genes, including *ERF1*, *PDF1.2a*, *LOX2*, *PR4*, *MYC2*, *LOX3* and *VSP2,* involved in the JA/ET signaling pathway for plant defense against necrotrophic pathogens. To date, few other

chromatin modifiers have been found to regulate the JA/ET signaling defense pathway. Ectopic overexpression of the histone deacetylase gene *HDA19* was shown to increase *ERF1* expression and enhance plant resistance to *A. brassicicola* (Zhou et al., 2005), and knockdown of *HDA6* resulted in impaired basal and JA-inducible expression of *PDF1.2a* and *VSP2* (Wu et al., 2008). However, histone acetylation levels at these defense genes were not investigated, and thus it is unclear whether *HDA19* and *HDA6* are directly or indirectly involved in regulation of the JA/ET pathway. More recently, it was reported that loss-of-function of *HISTONE MONOUBIQUITINATION1* (*HUB1*) increases plant susceptibility to necrotrophic fungal pathogens, however, the basal and inducible expression of *PDF1.2a* was unaffected in *hub1* mutant plants and it was suggested that *HUB1* regulates plant defense through an alternative pathway (Dhawan et al., 2009). Moreover, H2B ubiquitylation catalyzed by HUB1 has not been investigated with regards to plant defense against pathogens. The ATP-dependent chromatin remodeling factor gene *SPLAYED* (*SYD*) has been shown to be required for basal and inducible expression of *PDF1.2a* and *VSP2* in plant defense against necrotrophic fungal pathogens (Walley et al., 2008). Our study here demonstrates that H3K36 methylation at both *PDF1.2a* and *VSP2* is dynamic in response to fungal pathogen infection and MeJA treatment.

In wild-type plants, we uncovered the presence of a basal level of H3K36me3 at *PDF1.2a* and *VSP2*. Upon fungal pathogen infection or application of MeJA, the level of H3K36me3 increased, which positively correlates with induction of *PDF1.2a* and *VSP2* expression. In *sdg8-1* mutant plants, basal levels of H3K36me3 were low, and most interestingly, increases in H3K36me3 and induced expression of *PDF1.2a* and *VSP2* failed to occur in response to fungal infection or MeJA treatment. Changes in H3K36me1 levels were directly opposed to modifications in H3K36me3 in most cases examined. This is consistent with previous observations concerning different degrees of H3K36 methylation at floral

repressor genes and supports the idea that SDG8 is a histone methyltransferase responsible for converting H3K36me1 to H3K36me2 then H3K36me3 (Xu et al., 2008). Our results further suggest that the enzyme catalyzing H3K36me1 deposition is not involved in response to fungal pathogen infection or MeJA treatment. The particular importance of SDG8 in plant pathogen defense was also highlighted by the observation that *SDG8* expression is induced by fungal pathogen infection. Nevertheless, global levels of H3K36me3 in wild-type plants remained unchanged upon fungal pathogen infection or following MeJA treatment. Future experiments will be required to better understand how SDG8 is activated and/or recruited to specific genes in response to fungal infection or MeJA treatment.

Our work provides novel insights into the transcriptional regulation of *MKK* genes. Through phosphorylation cascades, MKKs play important roles at early steps of the SA, JA and ET defense signaling pathways (Asai et al., 2002; Takahashi et al., 2007; Zhang et al., 2007), and there is some evidence suggesting that they contribute to pathogen resistance (Asai et al., 2002). Knowledge of the mechanisms regulating *MKK* transcription remains scarce. We demonstrated that inducible expression of both *MKK3* and *MKK5* is dependent on SDG8-mediated H3K36me3. Epigenetic regulation of these early-acting defense genes might be advantageous, providing a more efficient way to trigger downstream events of the signaling pathways, however, further experiments will be needed to determine to what extent the *MKK3* and *MKK5* transcriptional differences in the *sdg8* mutant contribute to the reduced resistance against necrotrophic fungal pathogens. Strikingly, while *MKK5*, like the genes we characterized previously, showed reduced levels of expression and H3K36me3, *MKK3* conversely showed increased transcript and H3K36me3 levels in the unchallenged *sdg8-1* mutant compared to wild-type plants. This finding implies that in the absence of SDG8 another enzyme of yet unknown identity is activated/recruited to catalyze H3K36me3 at *MKK3*. The TrxG family in *Arabidopsis* is comprised of 12 *SDG* genes; so far the functions of

six of these *SDG* genes have been examined, and only SDG25, in addition to SDG8, was shown to be involved in H3K36 methylation (Berr et al., 2009). Future experiments will be required to examine whether *SDG25* and/or other uncharacterized *SDG* genes are involved in H3K36 methylation-associated regulation of *MKK* gene transcription.

The evidence provided in this study supports a model whereby SDG8 targets at least two distinct levels in the JA/ET signaling pathway in plant defense against necrotrophic fungal pathogens. SDG8 catalyzes H3K36me3 for basal and inducible expression of defense genes including *MKK5*, involved very early in the signaling pathway, and *PDF1.2a* and *VSP2*, at later stages in the defense response. The reduced expression in *sdg8-1* of *ERF1* and *MYC2*, two genes encoding central transcription factors that control a wide spectrum of downstream defense genes, is consistent with the accepted positive and negative control exerted by *MKK5* and *MKK3* over *ERF1* and *MYC2*, respectively. The implication of H3K36 methylation in regulation of a subset of genes, rather than a single target gene within the JA/ET defense pathway, is consistent with the necessity of multiple gene networks allowing for enhanced efficiency in plant defense. Based on our study, we propose that SDG8-mediated H3K36me3 establishes a favorable chromatin environment that may be considered as a memory mark of active transcription and is highly beneficial to plant survival.

MATERIALS AND METHODS

Biological materials and growth conditions

The *sdg8-1* and *sdg8-2* mutants in the Columbia (Col) ecotype were previously described (Zhao et al., 2005). For pathogen treatments, mutants and wild-type Col plants were grown on soil under 12 h light/12 h dark photoperiod in a growth chamber. *Alternaria brassicicola* (strain MUCL20297) and *Botrytis cinerea* (strain IMI169558) were grown and maintained as

described previously (La Camera et al., 2005).

SDG8p::GUS construct and plant transformation

The –2685 bp to –3 bp region relative to the ATG start codon of *SDG8* was amplified from wild-type genomic DNA by PCR using primers 5'-AATGCTACCTGATTCAAAGC-3' and 5'-AATGAGACGCTTCTTAAGC-3'. The PCR product was cloned into the pCRII-TOPO (Invitrogen, Cergy Pontoise, France) vector and sequenced to confirm the absence of errors. A 2655 bp *Hind*III-*Xba*I fragment of the *SDG8* promoter was subsequently cloned before the *GUS* coding region, replacing the *Hind*III-*Xba*I 35S promoter fragment in the binary vector pBI121 (Clontech, Saint-Germain-en-Laye, France). The resulting plasmid was introduced into *Agrobacterium tumefaciens* and used to transform Col plants using the floral-dip method (Clough and Bent, 1998). More than 30 independent transgenic lines were obtained and three representative lines were used for in depth analysis in this study.

Histochemical assays and microscopy

For GUS staining, freshly harvested plant material was collected and immediately vacuum-infiltrated for 15 min in GUS staining buffer (Jefferson et al., 1987) and incubated at 37°C for 3 to 15 h. Plant material was cleared in 70% ethanol and observed directly. The results presented here were reproducibly obtained from more than 3 independent transgenic lines.

For Trypan blue staining, leaves were harvested, stained and boiled for 1 min in lactophenol–trypan blue solution (Koch and Slusarenko, 1990) and cleared overnight in chloral hydrate solution (75 g of chloral hydrate dissolved in 30 ml of distilled water). Seedlings or organs of wild-type and mutant plants were examined using a LEICA MZ12 dissecting microscope (Leica, Rueil Malmaison, France). Higher magnification images and

histology sections were acquired with a Nikon Eclipse 800 microscope (Nikon, Paris, France). Images were processed with Adobe Photoshop 6.0 (Adobe Systems, San Jose, CA, USA).

Pathogen inoculation and JA treatment

Inoculation with *A. brassicicola* and *B. cinerea* and methyl jasmonate (MeJA) treatments were performed on 6-week-old mature vegetative plants. For *A. brassicicola* disease assays, two 5 µl droplets of spore suspension (5×10^5 spores/ml of water) were placed directly on the upper surface of the leaf. Prior to *B. cinerea* inoculation, two small holes were made with a needle on either side of the midrib before a 5 µl droplet of spore suspension (5×10^5 spores/ml of potato dextrose broth medium) was placed on each hole. Mock inoculations, without fungal spores, were also performed. Plants were then incubated in airtight translucent boxes to achieve saturating humidity. Typically, two inoculation sites per leaf were performed on 4 to 6 leaves of each plant.

For JA treatments, potted wild-type and mutant plants were placed into an airtight translucent container for 24 h to allow for acclimation before treatment with 10 µL of MeJA (95% purity; Sigma-Aldrich, Saint-Quentin, France) applied to cotton tips placed in the container.

***In planta* quantification of pathogen growth**

A. brassicicola and *B. cinerea* growth in infected plants was determined by relative quantification of fungal and plant DNA by means of quantitative PCR (qPCR) analysis. Total fungal and plant DNA was extracted as described (Gachon and Saindrenan, 2004) from 8 mm diameter leaf disks centered on the inoculation site at various time points before and after pathogen inoculation. Typically, leaf disks were pooled from at least 6 individual plants for each time point analysis. The relative quantity of *A. brassicicola* and *B. cinerea* was

calculated according to the abundance of the respective fungal *cutinase* gene (loci ABU03393 and Z69264, respectively), relative to *Arabidopsis*-specific *Actin2* DNA measured by qPCR. Analyses were performed in triplicates. Primer sequences are detailed in Table S8.

Camalexin measurement

For camalexin measurements, inoculated leaves were pooled from 6 individual plants at each time point after *A. brassicicola* inoculation, frozen in liquid nitrogen, ground to a fine powder with a mortar and pestle, and dissolved in 5 volumes of ice-cold 80% methanol. After centrifugation at 10,000 g for 20 min, the supernatants were separated on a HPLC system equipped with a RP C18 column (Novapak, 4 µm, 4.6 x 250 mm; Waters, Milford, MA, USA) using an increasing gradient of acetonitrile. Gradient conditions at a flow rate of 1 ml/min were as follows: 0 to 25% solvent B for 10 min, 25 to 60% for 30 min, 100% for 5 min followed by 100% solvent A for 8 min (solvent A, 10% acetonitrile in water; solvent B, 100% acetonitrile). Camalexin and fluorescent compounds were measured with a 474 detector (Waters) set at 315 nm excitation and 405 nm emission. Sinapoyl-malate abundance does not vary upon infection in leaves and was used as an internal standard for recovery. Camalexin amounts were calculated using a standard curve established with purified camalexin and an extinction coefficient of 14,000.

JA measurement

JA measurements were performed using ultra performance liquid chromatography coupled to tandem mass spectrometry (UPLC-MS/MS). Four volumes of ice-cold 90% methanol containing 330 µM methyl-dihydro-JA (Me-dhJA, Sigma-Aldrich), serving as an internal standard, were added to 100-150 mg of frozen leaf powder in a screw-capped tube containing glass beads. Material was ground twice for 30 sec with a Precellys 24 tissue homogenizer

(Bertin Technologies, Montigny-Le-Bretonneux, France). Homogenates were cleared by two successive centrifugations at 20,000 g and supernatants were saved for UPLC-MS analysis. Endogenous JA values were corrected according to Me-dhJA recovery. All analyses were performed using an Acquity UPLC system (Waters) coupled to a Quattro Premier XE triple quadrupole mass spectrometer equipped with an electrospray ionisation (ESI) source. Chromatographic separation was achieved using an Acquity UPLC BEH C_{18} column (100 x 2.1 mm, 1.7 µm) and Acquity UPLC BEH C_{18} pre-column (2.1 x 5 mm, 1.7 µm). The mobile phase consisted of (A) water/acetonitrile/formic acid (94.9/5/0.1, v/v/v), (B) acetonitrile/formic acid (99.9/0.1, v/v). The column was first equilibrated in 100% A, then a linear gradient was applied for 10 min to reach 100 % B, followed by an isocratic run with 100% B for 2 min before returning to initial conditions (100 % A) in 1 min. The total run time was 17 min. The column was operated at 28°C with a flow-rate of 0.45 ml/min (sample injection volume 3µl). Nitrogen was used as the drying and nebulizing gas. The nebulizer gas flow was set to approximately 50 L/h, and the desolvatation gas flow to 900 L/h. The interface temperature was set to 400°C and the source temperature to 135°C. The capillary voltage was set to 3.4 kV and the cone voltage and the ionization mode (positive and negative) were optimized for each molecule. The selected ion recording (SIR) MS mode was used to determine parent mass transition of JA (m/z: 209 in negative mode); methyl-dihydro jasmonic acid (m/z: 227 in positive mode) with a cone voltage of 25 V for all the components. JA fragmentation was performed by collision-induced dissociation with argon at 1.0×10^{-4} mbar using multiple reaction monitoring (MRM). The collision energy was set to 20 V and the 209>59 transition was used for JA as previously described (Pan et al., 2008). The combination of chromatographic retention time, parent mass and unique fragment ions analysis was used to selectively monitor JA. Low mass and high mass resolution was 15 for both mass analyzers, ion energies 1 and 2 were 0.5 V, entrance and exit potential were 2 V

and 1 V, and detector (multiplier) gain was 650 V. Data acquisition and analysis was performed with the MassLynx software (version 4.1; Waters).

RNA isolation and reverse transcription

Total RNA was extracted from plant tissue with Trizol reagent (Molecular Research Center Inc., Cincinnati, OH, USA). Three tissue types were used in this study. For fungal infection of 6-week-old plants, leaf disks (8 mm diameter) centered on the inoculation site were pooled from at least 6 individual plants for each sample. The use of leaf disks of uniform size aims to minimize any possible effects introduced by size variations among individual plants and between the wild-type Col and *sdg8* mutant. For MeJA treatment of 6-week-old plants, aerial tissues from 6 individual plants were collected for each sample. For MeJA treatment of 10-day-old seedlings, at least 100 individual seedlings grown in 4 small pots (7 cm x 7 cm) were pooled for each sample. For cDNA synthesis, 2 μg of total RNA was treated first with 2 units of DNase I (Promega, France, Charbonnières-les-Bains, France) and then reverse transcribed in a 40 μl total volume with 2 μM oligo(dT)$_{20}$, 0.5 mM dNTPs, 5 mM DTT, and 200 units of SuperScript III reverse transcriptase (Invitrogen). The resulting cDNA was used for qPCR analysis.

Histone methylation analysis

Histone methylation was analyzed using western blot and chromatin immunoprecipitation (ChIP). These methods require more starting material than the previously described experiments, and thus leaf disks were pooled from at least 12 individual plants for each sample. Specific antibodies used in this study were anti-H3 (05-499; Millipore, Molsheim, France), anti-monomethyl-H3K36 (ab9048; AbCam, Paris, France), anti-trimethyl-H3K36 (ab9050; AbCam), and anti-trimethyl-H3K27 (07-449; Millipore). Western blot analysis was

performed as previously described (Xu et al., 2008) and ChIP was performed with the following modifications. Chromatin was sheared with a BIORUPTOR (Cosmo Bio Co. Ltd., Tokyo, Japan) sonicator twice for 15 min with a 50% duty cycle and high power output, in order to obtain 200–1000 bp DNA fragments. Chromatin was immunoprecipitated with specific antibodies together with protein A magnetic beads (Millipore). Following elution with Proteinase K (Invitrogen), DNA was recovered using Magna ChIP spin filters (Millipore). ChIP experiments using protein A magnetic beads without the addition of antibody were carried out as negative controls. The resulting ChIP DNA was subjected to qPCR analysis.

Quantitative real-time PCR analysis

qPCR analyses were performed on cDNA or ChIP products with gene-specific primers designed using the Light Cycler Probe Design 2 program (Roche, Meylan, France) in a final volume of 10 μl SYBR Green Master mix using a Light Cycler 480 II instrument (Roche) according to the manufacturer's instructions.

For qPCR analysis of cDNA products, several conventionally used reference genes were evaluated for their respective stability under our experimental conditions using geNorm (Vandesompele et al., 2002) and Norm Finder (Andersen et al., 2004), and based on these results, the housekeeping genes *EXP* (At4g26410), *GAPDH* (At1g13440) and *TIP41* (At4g34270) were selected for use as internal references. After qPCR amplification, melting curve analysis was performed to verify amplification of a single PCR product. The target gene expression level was normalized against internal reference genes, averaged over triplicates, and shown as a relative value.

For qPCR analysis of ChIP products, enrichment for H3K36 mono- or tri-methylation was determined using the Pfaffl equation (Pfaffl, 2001), using *ACTIN2/7* (At5g09810) and

TUB2 (At5g62690) as reference genes. Enrichment for H3K27 tri-methylation was similarly determined using *FUSCA3* (At3g26790) as a reference.

Gene-specific primer sequences used for qPCR of cDNA or ChIP products are listed in Table S8.

ACKNOWLEDGMENTS

REFERENCES

Alvarez-Venegas R, Abdallat AA, Guo M, Alfano JR, Avramova Z (2007) Epigenetic control of a transcription factor at the cross section of two antagonistic pathways. Epigenetics **2:** 106-113

Alvarez-Venegas R, Avramova Z (2005) Methylation patterns of histone H3 Lys 4, Lys 9 and Lys 27 in transcriptionally active and inactive *Arabidopsis* genes and in *atx1* mutants. Nucleic Acids Res **33:** 5199-5207

Andersen CL, Jensen JL, Orntoft TF (2004) Normalization of real-time quantitative reverse transcription-PCR data: a model-based variance estimation approach to identify genes suited for normalization, applied to bladder and colon cancer data sets. Cancer Res **64:** 5245-5250

Asai T, Tena G, Plotnikova J, Willmann MR, Chiu WL, Gomez-Gomez L, Boller T, Ausubel FM, Sheen J (2002) MAP kinase signalling cascade in *Arabidopsis* innate immunity. Nature **415:** 977-983

Berr A, Xu L, Gao J, Cognat V, Steinmetz A, Dong A, Shen WH (2009) *SET DOMAIN GROUP25* encodes a histone methyltransferase and is involved in *FLOWERING LOCUS C* activation and repression of flowering. Plant Physiol **151:** 1476-1485

Boter M, Ruiz-Rivero O, Abdeen A, Prat S (2004) Conserved MYC transcription factors play a key role in jasmonate signaling both in tomato and *Arabidopsis*. Genes Dev **18:** 1577-1591

Cazzonelli CI, Cuttriss AJ, Cossetto SB, Pye W, Crisp P, Whelan J, Finnegan EJ, Turnbull C, Pogson BJ (2009) Regulation of carotenoid composition and shoot branching in *Arabidopsis* by a chromatin modifying histone methyltransferase, SDG8. Plant Cell **21:** 39-53

Cazzonelli CI, Roberts AC, Carmody ME, Pogson BJ (2010) Transcriptional control of *SET DOMAIN GROUP8* and *CAROTENOID ISOMERASE* during *Arabidopsis* development. Mol. Plant **3:** 174-191

Clough SJ, Bent AF (1998) Floral dip: a simplified method for *Agrobacterium*-mediated transformation of *Arabidopsis thaliana*. Plant J **16:** 735-743

De Vos M, Van Oosten VR, Van Poecke RM, Van Pelt JA, Pozo MJ, Mueller MJ, Buchala AJ, Metraux JP, Van Loon LC, Dicke M, Pieterse CM (2005) Signal signature and transcriptome changes of *Arabidopsis* during pathogen and insect attack. Mol Plant Microbe Interact **18:** 923-937

Dhawan R, Luo H, Foerster AM, Abuqamar S, Du HN, Briggs SD, Mittelsten Scheid O, Mengiste T (2009) HISTONE MONOUBIQUITINATION1 interacts with a subunit of the mediator complex and regulates defense against necrotrophic fungal pathogens in *Arabidopsis*. Plant Cell **21:** 1000-1019

Dong G, Ma DP, Li J (2008) The histone methyltransferase SDG8 regulates shoot branching in Arabidopsis. Biochem Biophys Res Commun **373:** 659-664

Ferreira RB, Monterio S, Freitas R, Santos CN, Chen Z, Batista LM, Durate J, Borges A, Teixeira AR (2007) The role of plant defence proteins in fungal pathogenesis. Molecular Plant Pathology **5:** 677-700

Gachon C, Saindrenan P (2004) Real-time PCR monitoring of fungal development in *Arabidopsis thaliana* infected by *Alternaria brassicicola* and *Botrytis cinerea*. Plant Physiol Biochem **42:** 367-371

Glazebrook J (2005) Contrasting mechanisms of defense against biotrophic and necrotrophic pathogens. Annu Rev Phytopathol **43:** 205-227

Glazebrook J, Chen W, Estes B, Chang HS, Nawrath C, Metraux JP, Zhu T, Katagiri F (2003) Topology of the network integrating salicylate and jasmonate signal transduction derived from global expression phenotyping. Plant J **34:** 217-228

Grini PE, Thorstensen T, Alm V, Vizcay-Barrena G, Windju SS, Jorstad TS, Wilson ZA, Aalen RB (2009) The ASH1 HOMOLOG 2 (ASHH2) histone H3 methyltransferase is required for ovule and anther development in *Arabidopsis*. PLoS One **4:** e7817

He Y (2009) Control of the transition to flowering by chromatin modifications. Mol Plant **2:** 554-564

Jefferson RA, Kavanagh TA, Bevan MW (1987) GUS fusions: beta-glucuronidase as a sensitive and versatile gene fusion marker in higher plants. EMBO J. **6:** 3901-3907

Jones JD, Dangl JL (2006) The plant immune system. Nature **444:** 323-329

Kim JM, To TK, Ishida J, Morosawa T, Kawashima M, Matsui A, Toyoda T, Kimura H, Shinozaki K, Seki M (2008) Alterations of lysine modifications on the histone H3 N-tail under drought stress conditions in *Arabidopsis thaliana*. Plant Cell Physiol **49:** 1580-1588

Kim SY, He Y, Jacob Y, Noh YS, Michaels S, Amasino R (2005) Establishment of the vernalization-responsive, winter-annual habit in *Arabidopsis* requires a putative histone H3 methyl transferase. Plant Cell **17:** 3301-3310

Koch E, Slusarenko A (1990) *Arabidopsis* is susceptible to infection by a downy mildew fungus. Plant Cell **2:** 437-445

Kwon CS, Lee D, Choi G, Chung WI (2009) Histone occupancy-dependent and -independent removal of H3K27 trimethylation at cold-responsive genes in *Arabidopsis*. Plant J **60:** 112-121

La Camera S, Geoffroy P, Samaha H, Ndiaye A, Rahim G, Legrand M, Heitz T (2005) A pathogen-inducible patatin-like lipid acyl hydrolase facilitates fungal and bacterial host colonization in *Arabidopsis*. Plant J **44:** 810-825

Lorenzo O, Chico JM, Sanchez-Serrano JJ, Solano R (2004) *JASMONATE-INSENSITIVE1* encodes a MYC transcription factor essential to discriminate between different jasmonate-regulated defense responses in *Arabidopsis*. Plant Cell **16:** 1938-1950

Lorenzo O, Piqueras R, Sanchez-Serrano JJ, Solano R (2003) ETHYLENE RESPONSE FACTOR1 integrates signals from ethylene and jasmonate pathways in plant defense. Plant Cell **15:** 165-178

Pan X, Welti R, Wang X (2008) Simultaneous quantification of major phytohormones and related compounds in crude plant extracts by liquid chromatography-electrospray tandem mass spectrometry. Phytochemistry **69:** 1773-1781

Pfaffl MW (2001) A new mathematical model for relative quantification in real-time RT-PCR. Nucleic Acids Res **29:** 2002-2007

Pien S, Grossniklaus U (2007) Polycomb group and trithorax group proteins in *Arabidopsis*. Biochim Biophys Acta **1769:** 375-382

Pitzschke A, Schikora A, Hirt H (2009) MAPK cascade signalling networks in plant defence. Curr Opin Plant Biol **12:** 421-426

Shen WH, Xu L (2009) Chromatin remodeling in stem cell maintenance in *Arabidopsis thaliana*. Mol Plant **2:** 600-609

Strahl BD, Allis CD (2000) The language of covalent histone modifications. Nature **403:** 41-45

Takahashi F, Yoshida R, Ichimura K, Mizoguchi T, Seo S, Yonezawa M, Maruyama K, Yamaguchi-Shinozaki K, Shinozaki K (2007) The mitogen-activated protein kinase cascade MKK3-MPK6 is an important part of the jasmonate signal transduction pathway in *Arabidopsis*. Plant Cell **19:** 805-818

Teige M, Scheikl E, Eulgem T, Doczi R, Ichimura K, Shinozaki K, Dangl JL, Hirt H (2004) The MKK2 pathway mediates cold and salt stress signaling in *Arabidopsis*. Mol Cell **15:** 141-152

Thomma BP, Eggermont K, Penninckx IA, Mauch-Mani B, Vogelsang R, Cammue BP, Broekaert WF (1998) Separate jasmonate-dependent and salicylate-dependent defense-response pathways in *Arabidopsis* are essential for resistance to distinct microbial pathogens. Proc Natl Acad Sci U S A **95:** 15107-15111

Thomma BP, Nelissen I, Eggermont K, Broekaert WF (1999) Deficiency in phytoalexin production causes enhanced susceptibility of *Arabidopsis thaliana* to the fungus *Alternaria brassicicola*. Plant J **19:** 163-171

Turner BM (2000) Histone acetylation and an epigenetic code. Bioessays **22:** 836-845

Vandesompele J, De Preter K, Pattyn F, Poppe B, Van Roy N, De Paepe A, Speleman F (2002) Accurate normalization of real-time quantitative RT-PCR data by geometric averaging of multiple internal control genes. Genome Biol **3:** RESEARCH0034

Walley JW, Rowe HC, Xiao Y, Chehab EW, Kliebenstein DJ, Wagner D, Dehesh K (2008) The chromatin remodeler SPLAYED regulates specific stress signaling pathways. PLoS Pathog **4:** e1000237

Wu K, Zhang L, Zhou C, Yu CW, Chaikam V (2008) *HDA6* is required for jasmonate response, senescence and flowering in *Arabidopsis*. J Exp Bot **59:** 225-234

Xing Y, Jia W, Zhang J (2008) AtMKK1 mediates ABA-induced CAT1 expression and H2O2 production via AtMPK6-coupled signaling in *Arabidopsis*. Plant J **54:** 440-451

Xu L, Zhao Z, Dong A, Soubigou-Taconnat L, Renou JP, Steinmetz A, Shen WH (2008) Di- and tri- but not monomethylation on histone H3 lysine 36 marks active transcription of genes involved in flowering time regulation and other processes in *Arabidopsis thaliana*. Mol Cell Biol **28:** 1348-1360

Zhang X, Dai Y, Xiong Y, DeFraia C, Li J, Dong X, Mou Z (2007) Overexpression of *Arabidopsis MAP kinase kinase 7* leads to activation of plant basal and systemic acquired resistance. Plant J 52: 1066-1079

Zhao Z, Yu Y, Meyer D, Wu C, Shen WH (2005) Prevention of early flowering by expression of *FLOWERING LOCUS C* requires methylation of histone H3 K36. Nat Cell Biol **7:** 1256-1260

Zhou C, Zhang L, Duan J, Miki B, Wu K (2005) *HISTONE DEACETYLASE19* is involved in jasmonic acid and ethylene signaling of pathogen response in *Arabidopsis*. Plant Cell **17:** 1196-1204

FIGURE LEGENDS

Figure 1. Expression pattern of *SDG8p::GUS* in transgenic plants. (A) 8-day-old seedling. (B) Close-up of the shoot tip of an 8-day-old seedling. (C) Part of leaf margin (insert shows a whole leaf). (D) Base of shoot branches and cauline leaf petiole. (E) Open flower. (F) Young silique. (G) Mature leaf wounded immediately prior to GUS staining. (H) Leaf inoculated with *B. cinerea* at 3 days post-inoculation (dpi) before (left) and after GUS staining (right). (I) Leaf inoculated with *A. brassicicola* at 5 dpi before (left) and after GUS staining (right). (J) Relative level of endogenous *SDG8* expression after *B. cinerea* (grey bar) or mock (white bar) inoculation. Data represents the mean ± SD of triplicates. Asterisks indicate a significant difference between Col and *sdg8-1* at $P<0.05$ (two sided *t*-test). Similar results were obtained in two independent experiments (refer to Supplemental Table S1).

Figure 2. Comparison of pathogen-responsive phenotypes between mutant *sdg8* and wild-type Col plants. (A) Plant disease symptoms observed at 3 dpi on leaves inoculated with *B. cinerea*. Mock inoculation is shown as control. White arrows indicate small lesions caused by *B. cinerea* on wild-type Col leaves. Note that more severe lesions occur in both *sdg8-1* and *sdg8-2* mutants. (B) Mean leaf lesion diameter at 3 dpi with *B. cinerea* (n ≥ 20; ± SEM). (C) Visualization of fungal growth and cell death in Col and *sdg8-1* leaves after trypan blue staining at 3 dpi with *B. cinerea*. Asterisk indicates a significant difference between Col and *sdg8-1* at $P<0.05$ (two sided *t*-test). (D) Quantification of *in planta* growth of *B. cinerea*. qPCR was used to analyze the relative genomic DNA level of *B. cinerea cutinase-A* compared to *Arabidopsis Actin2* (*Bo cut-A / At ACT*). Data represents the mean ± SD of triplicates. (E) Plant disease symptoms observed at 5 dpi on leaves inoculated with *A. brassicicola*. White arrows indicate small lesions observed on Col leaves. (F) Mean leaf lesion diameter at 2 and 5

dpi with *A. brassicicola* (n ≥ 20; ± SEM). (G) Quantification of *in planta* growth of *A. brassicicola*. qPCR was used to analyze the relative genomic DNA level of *A. brassicicola cutinase* compared to *Arabidopsis Actin2* (*Alt cutab1 / At ACT*). Data represents the mean ± SD of triplicates.

Figure 3. Comparison of camalexin accumulation and defense marker gene expression in response to pathogen infection in mutant *sdg8-1* and wild-type Col plants. (A) Relative levels of camalexin in response to *A. brassicicola* infection in *sdg8-1* and Col plants. Camalexin values are presented relative to average wild-type levels at time point 0 (set as 1). Data represents the mean ± SEM of triplicates. (B) Simplified model for the regulation of plant defense networks in response to necrotrophic pathogen infection. Genes (*in italics*) involved in the jasmonate (JA) and ethylene (ET) signaling pathways, as well as MAPK kinase genes and their corresponding phophorylation cascade (arrows with filled head) are defined along the text. Positive (arrows with empty head) and negative (bars) regulations are depicted. (C) Relative expression levels of *PDF1.2a* and *VSP2* in *sdg8-1* and Col leaves in response to *A. brassicicola* inoculation. Gene expression values are presented relative to average wild-type levels at time point 0 (set as 1). Data represents the mean ± SD of triplicates. Asterisks indicate a significant difference between Col and *sdg8-1* at *P*<0.05 (two sided *t*-test). Similar results were obtained in two independent experiments (refer to Supplemental Table S2).
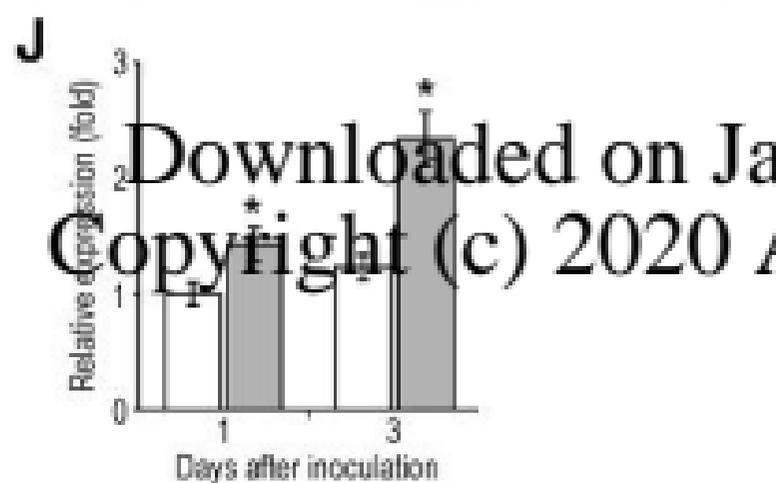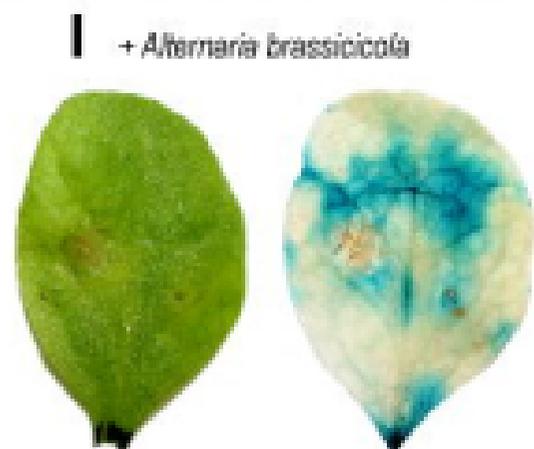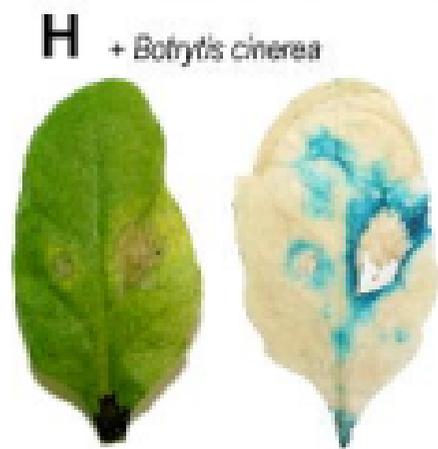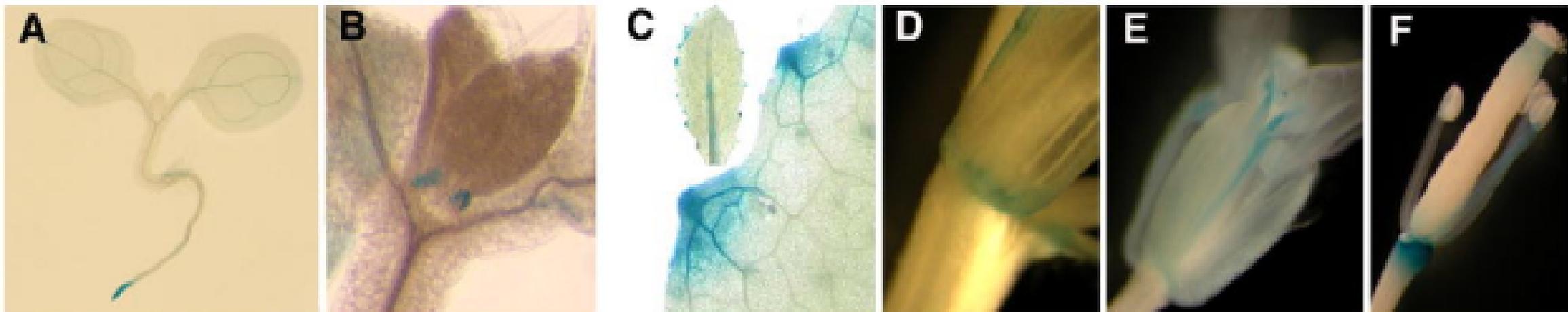
Figure 4. Comparison of JA accumulation and expression of JA/ET-responsive genes in mutant *sdg8-1* and wild-type Col plants. (A) Endogenous JA levels were measured by UPLC-MS using *sdg8-1* and Col leaves from plants inoculated with *A. brassicicola*. Data represents the mean ± SD of triplicates. (B) Relative expression levels of JA/ET pathway
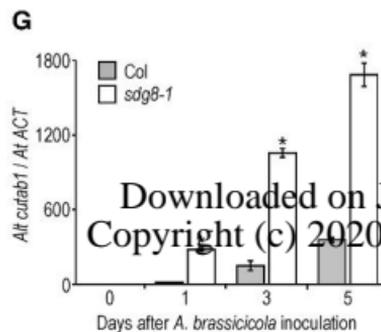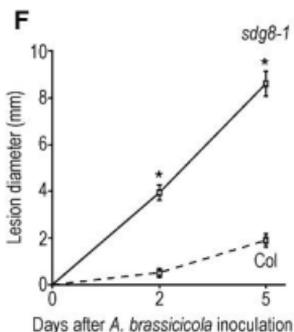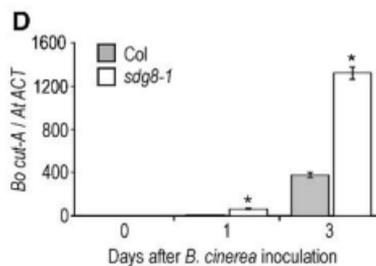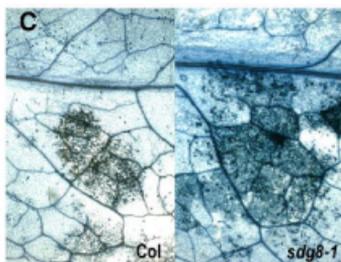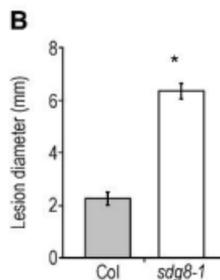
genes in *sdg8-1* and Col leaves in response to treatment with exogenously applied MeJA. Gene expression values are presented relative to average wild-type levels at time point 0 (set as 1). Data represents the mean ± SD of triplicates. Asterisks indicate a significant difference between Col and *sdg8-1* at $P<0.05$ (two sided *t*-test). Similar results were obtained in two independent experiments (refer to Supplemental Table S4).
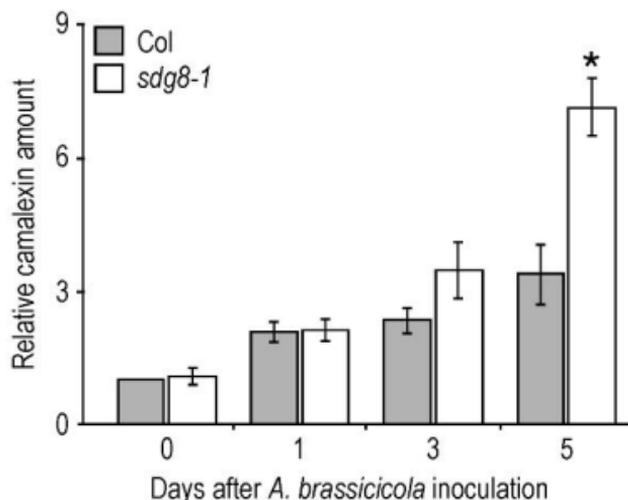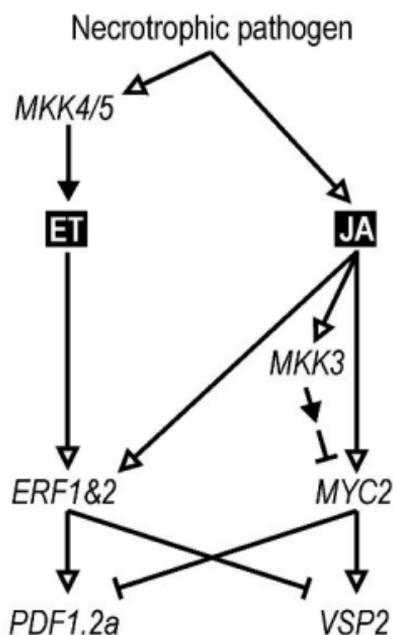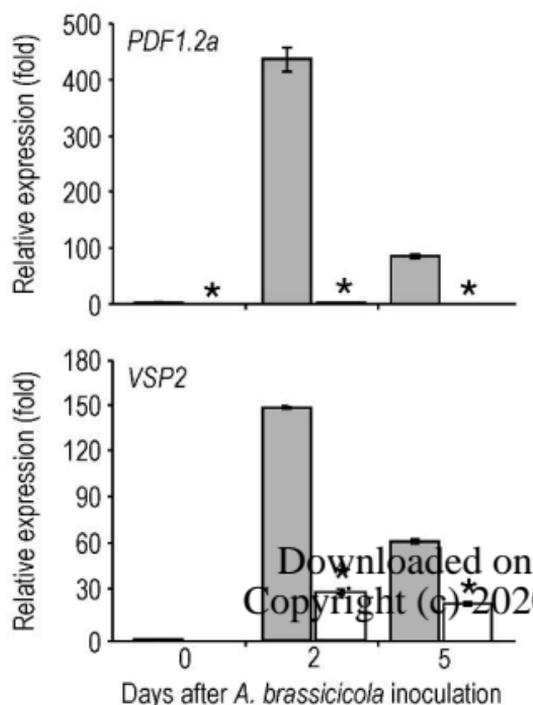
Figure 5. Analysis of histone methylation at defense marker genes in response to pathogen infection in mutant *sdg8-1* and wild-type Col plants. Chromatin immunoprecipitation analysis was used to determine the relative levels of H3K36me3, H3K36me1 and H3K27me3 before (white bar) and 2 days after *A. brassicicola* inoculation (black bar) of 6-week-old Col and *sdg8-1* plants at indicated regions of *PDF1.2a* and *VSP2*. Data represents the mean ± SD of triplicates. Similar results were obtained in two independent experiments (refer to Supplemental Table S6). Amplified regions (named a to d) are indicated below each gene, which is represented by a white box for the coding region and grey boxes for the 5' and 3' untranslated regions.

Figure 6. Expression and H3K36 methylation levels of MAPK kinase genes in response to pathogen infection in mutant *sdg8-1* and wild-type Col plants. (A, B) Relative expression levels of *MKK3* and *MKK5* after *A. brassicicola* inoculation and exogenous MeJA treatment. Gene expression values are presented relative to average wild-type levels at time point 0 (set as 1). Data represents the mean ± SD of triplicates. Asterisks indicate a significant difference between Col and *sdg8-1* at $P<0.05$ (two sided *t*-test). Similar results were obtained in two independent experiments (refer to Supplemental Tables S2 and S4). (C) Relative levels of H3K36me3 and H3K36me1 before (white bar) and 2 days after *A. brassicicola* inoculation (black bar) of 6-week-old Col and *sdg8-1* plants at indicated regions of *MKK3* and

MKK5. Data represents the mean ± SD of triplicates. Similar results were obtained in two independent experiments (refer to Supplemental Table S6). Amplified regions (named e to j) are indicated below each gene, which is represented by a white box for the coding region and grey boxes for the 5' and 3' untranslated regions.
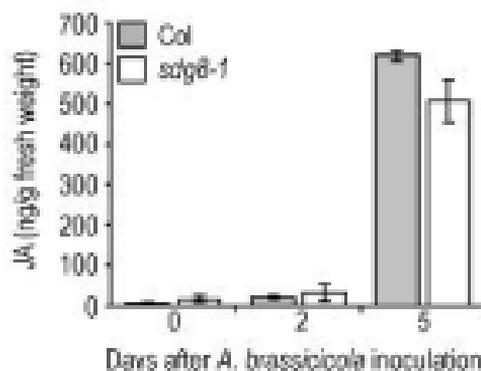
A B C D E F

G H + *Botrytis cinerea* I + *Alternaria brassicicola*

Relative expression (fold)

Days after inoculation
1 3

A + mock + *B. cinerea* + mock + *B. cinerea* + mock + *B. cinerea*

Col sdg8-1 sdg8-2

B
Lesion diameter (mm)

Col sdg8-1

C
Col sdg8-1

D
Col sdg8-1

Bo cutA-1 / At ACT

Days after *B. cinerea* inoculation

E + *A. brassicicola*

Col sdg8-1

F
Lesion diameter (mm)

sdg8-1

Col

Days after *A. brassicicola* inoculation

G
Col sdg8-1

Alt cutab1 / At ACT

Days after *A. brassicicola* inoculation

A

Relative camalexin amount

Col
sdg8-1

Days after *A. brassicicola* inoculation

B

Necrotrophic pathogen

MKK4/5

ET

JA

MKK3

ERF1&2

MYC2

PDF1.2a

VSP2

C

PDF1.2a

Relative expression (fold)

VSP2

Relative expression (fold)

Days after *A. brassicicola* inoculation

A

JA (ng/g fresh weight) — Col, sdg8-1

Days after *A. brassicicole* inoculation

B

ERF1
Relative expression (fold)
0, 8, 24, 48
Hours after MeJA treatment

MYC2
Relative expression (fold)
0, 8, 24, 48
Hours after MeJA treatment

PDF1.2a
Relative expression (fold)
0, 8, 24, 48
Hours after MeJA treatment

VSP2
Relative expression (fold)
0, 8, 24, 48
Hours after MeJA treatment